Filtration of Liquid Aerosols on Wettable Fibrous Filters

Igor E. Agranovski and Roger D. Braddock
Environmental Sciences, Griffith University, Nathan, Australia 4111

Liquid aerosols produced in many manufacturing and refining processes need to be filtered from the exhaust streams. Where wettable fibers are used in the filters, the aerosol liquid collects on the fibers. Observation shows that thin films develop on the fibers, and the liquid drains down the fibers under the action of gravity. A model is developed for the flow of liquid in these films, and careful experimentation confirms the nature and importance of the flow pattern. The resultant overall efficiencies of the filter are also calculated from a theoretical analysis and compared with the results of experimentation using counting techniques. The theoretical and experimental results agree excellently for the range of aerosol sizes that are detectable by laser diffraction and cascade impactor techniques.

Introduction

Air quality is becoming an important environmental factor, particularly in relation to environmental and health concerns. Filtration processes are used to control the particulate fluxes in exhaust streams from many industrial, chemical, and mining operations. Filtration processes and their management have long been the subject of research at both experimental and theoretical levels. [Davies (1973) provides an overview of the history of the subject.] The particle separation and pressure drop data for a fresh filter can be calculated using classical filtration theory (Hinds, 1982; Brown, 1993). In practical situations, this theory can be applied only to a fresh filter or for only the early stages of filtration. Even after a short period of running, deposits build up on the fibers, the filter becomes clogged, and important changes may take place to the flow field which considerably alter the filtering characteristics. Sometimes, especially for highly concentrated streams, the alterations are so significant that filters which have been designed according to classical theory operate poorly in real industrial processes.

The filtration of liquid particles is important in the chemical industry, particularly where the waste liquid may be highly toxic or corrosive, such as sulfuric acid. In this case, it may be possible to design a self-cleaning filter whereby the liquid particles are collected on the filter, but then drain down the filter to some collecting device. Such a self-cleaning filter can remain operational and near its design specifications for an almost indefinite period. Operational and maintenance costs are substantially reduced.

The literature contains only a few contributions relating to the filtration of liquid aerosols by fiber filters. Fairs (1958) described the mechanisms operating in the filtration of fine mists and also considered the high efficiencies which could be obtained using fibrous filters. Eriksson et al. (1992) also considered the adhesive forces between the fibers of a filter as the collection of an aerosol occurred on the filter. Mohrmann (1970) described the way in which liquid aerosols settled onto a fiber filter. Eriksson et al. (1992) and Mohrmann (1992) did not measure the efficiency of the filtration processes, and did not recognize the role of the various properties of the filter, aerosol, and gas stream. Kircsh (1978) did perform experiments to look at the increase in the pressure drop across the filter, due to the buildup of dendritic structures on a model filter.

Payet et al. (1990) performed some measurements of the performance of glass fiber filters loaded with submicrometer aerosols of oil. The results showed an increase in pressure drop with load and a reduction of penetration when the load was sufficient to cause a 20% increase in pressure drop. At higher loads, the penetration was increased by a factor of 2

Correspondence concerning this article should be addressed to I. E. Agranovski.

when the pressure drop was doubled and by a factor of 4 when it was tripled.

Various parameters of the filter and exhaust stream need to be considered. These include the physical and chemical properties of the waste liquid and the physical parameters of the carrier gas (such as temperature, velocity, and moisture content). However, the wettability of a fiber is one of the most important parameters of liquid aerosol filtration (Agranovski and Braddock, 1996). Liquids will adhere to wettable fibers and enhance the capture characteristics of the filtering device with respect to liquid particles.

The objectives of this article are to investigate the nature of the filtration processes by wettable fibers in the filter, and to assess the effects of the filtration efficiencies. Observations of the relevant processes are made to provide a broad overview of the operation of the filter. More detailed experiments are also described and measurements are reported on the structure of the water films on the wettable fibers. Models of the filtration efficiency are constructed and compared with observations.

Laboratory Plant and Preliminary Observations

The experimental program required the design and construction of a suitable laboratory plant which permitted the mounting of various measuring devices at several points in the flow path. The main components of the laboratory plant are:

- Centrifugal fan supplying air at rates up to 1.2 m^3/s
- Aerosol generator (polydisperse) providing water drops in the size range 0.1–20 μm
- Scrubber or plate tower with recirculating water which can be used to control the temperature
- Filter assembly to hold a variable number of filter frames. The frames are mounted vertically and are 1 m high and 0.3 m wide.

The filter box also incorporated an observation window so that the behavior of the liquid aerosol on the filter could be directly observed. Water was used to form the aerosol particles.

Instrumentation of the plant included measurement of temperature, humidity and flow velocity, as well as the particle-size distributions of the aerosol before and after passage through the filter. These particle-size distributions were measured using both a laser particle-size analyzer (Malvern, UK) in combination with particle counter and a cascade impactor. The design of the laboratory plant is described in Agranovski (1995).

The observations and experimental work were performed with filters manufactured from fiberglass, which is wettable by water. The diameter of the fiber was 7 μm, the thickness of the filter was 6 mm, the length of the filter (and of the fibers) was 1 m, the width of the filter was 30 cm, and the packing density was 3%.

In manufacture, the filters are constructed by laying parallel cylindrical fibers together and then pressing to achieve the final packing density. Close examination of the filters confirmed this general structure and orientation with some additional structural complexity. The packing density of 3% was confirmed by weighing the filter pads, measuring their physical dimensions and using the density of fiberglass to calculate the packing density.

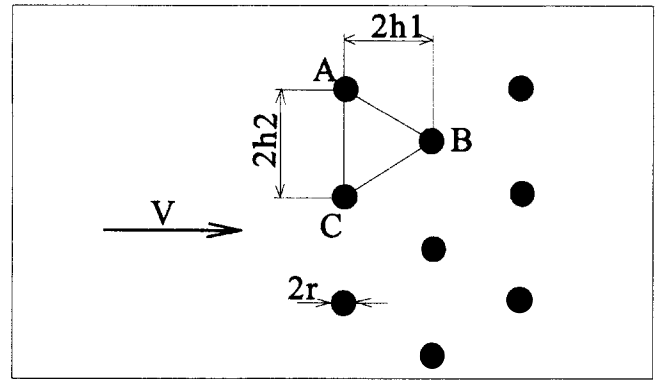

Figure 1. Assumed regular cross-sectional arrangement of fibers.

The physical structure of the filter, its packing density and the physical dimensions of the fibers permit the estimation of the number of parallel cylinders (or fibers) in the filter. The filter was assumed to be a system of parallel vertical cylinders in a regular hexagonal packing arrangement (Figure 1). Now, the packing density of the filter is 3%, and the ratio of the half cross-section area of the fiber by the cross-section area of the equilateral triangle ABC in Figure 1 is 0.03. Thus, using the notation in Figure 1

$$2h_2 \approx 38.5\ \mu\text{m}; \quad 2h_1 = 38.5\cos 30^\circ \approx 33.34\ \mu\text{m}.$$

This gives the number of rows of cylinders as being equal to 180. The number of cylinders in each row is 7,792 and the total number of the fibers in the filter (1,000 mm × 300 mm × 6 mm) is 1,402,560. Thus, the filter is described fully.

Some preliminary observations were carried out using the observation window in the filter box. The objective was to obtain an overview of the filtration process and to provide guidance for the more precise experimental and theoretical work. These observations were conducted with an air face velocity of 1.0 m/s, a humidity of 85%, a temperature of 20°C, and a water aerosol concentration of 3 g/m^3. The filter was dry when inserted in the filter box, and was located with the fibers being vertical.

At the beginning of the filtering process, it was observed that the aerosols collected by a filter remain on its surface as drops and grow as they coalesce with new incoming droplets. When the coalescing drop becomes quite large and the force of gravity exceeds the adhesion force, the drop is drained down. During this motion, it was observed that the draining drop wets other fibers on its way down, and after some period of time, liquid covers all the fibers of the filter.

The first drops drained from the surface of the filter some 47 s after the aerosol flow was started (stage 1). During the second stage (the next four minutes), the number of drops was increasing relatively smoothly. During the third stage (the next 6 min), the number of drops on the filter was approximately constant or stable (see Figure 2a). At that moment, a significant part of the filter was blocked by the drops.

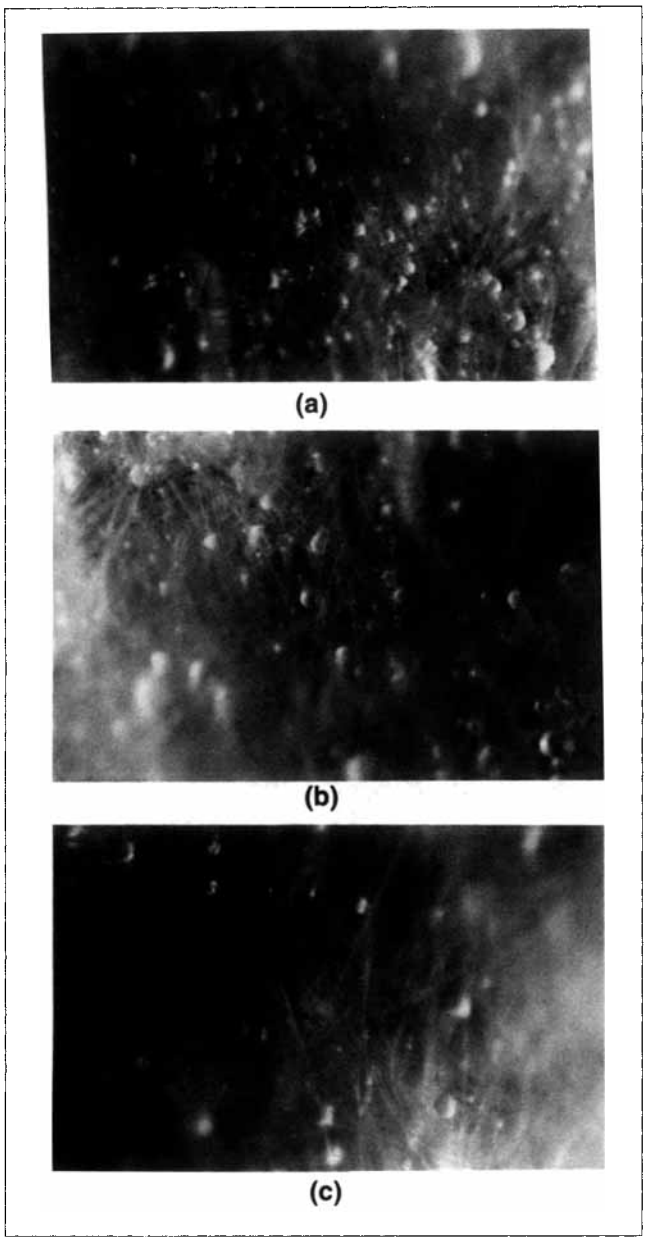

Figure 2. Surface of the filter.

(a) At Stage 3 after some 10 min of filtration; (b) during Stage 4 after some 15 min of filtration; (c) near end of Stage 4, after some 32 min of filtration.

During stage 4 (the next 32 min), the number of droplets was decreasing (Figures 2b and 2c) and the last droplet disappeared at the end of this stage. At this point in time (some 43 min after starting the plant), each fiber was covered by a liquid film and all of the fibers were separated from each other. From this moment on and with the plant running, only a tapered filmy flow of water was observed on each fiber. This flow is called the equilibrium film.

Some 10 to 15 min after the end of stage 4, the fan and the aerosol generator were turned off and the filter was left to dry. Liquid was draining along each fiber for the next 48 min, and then this flow ceased. All the fibers were still wet with a film of water, but further drainage of water did not occur; this film is called the residual film. This residual film is the film of water remaining on a fiber after drainage of excess water, and represents a static balance between gravity and adhesion forces.

To observe the behavior of drops on the fiber, a further experiment was carried out in which a single fiber was fixed stationary in the holder and located vertically in the hermetically sealed chamber. Droplets of water were supplied through the atomizer until some of them have settled on the fiber. To prevent the evaporation of water from the film's surface, the experiment was carried out in the chamber with 100% relative humidity.

The droplets spread along the wettable fiber and created a thin film which covered the fiber (Figures 3a and 3b). Excess water drained down the fiber, but a thin equilibrium film remains over the fiber surface. This film increases the effective diameter of the fiber for the capture of aerosol particles and affects the efficiency of the filtration process.

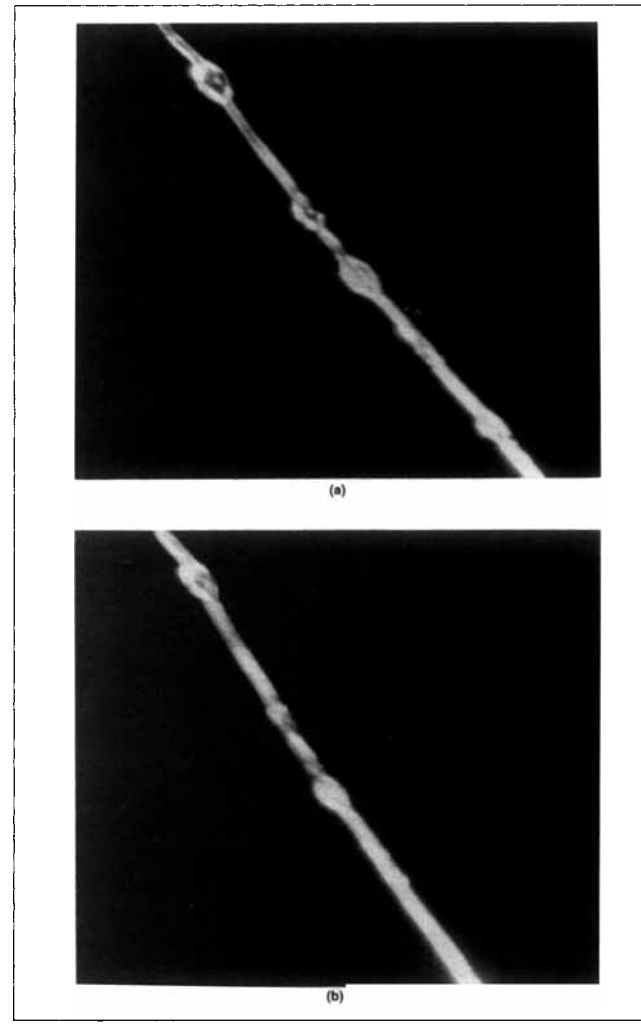

Figure 3. Spreading of droplets along the single fiber located in the hermetically sealed chamber.

(a) 5 min. after settling (generator is switched off); (b) 10 min after settling (generator is switched off).

Theoretical Studies

During the filtration process, there is a continuous capture of aerosol particles into the liquid film covering each fiber. The film also drains under gravity. The equilibrium film represents the balance between the capture of aerosol particles and drainage down the fiber, the equilibrium film is thicker than the residual film. The shape and thickness of the equilibrium film can be derived from a modeling analysis of the flow of water in the film.

Now consider the equilibrium film of water flowing down each fiber which is of length L_F: here, $L_F = 1$ m. The inter-fiber spacings are of the order of 38 μm and the "tapering" of the film is very small; the surface of the film being almost parallel to the fiber (see Figure 4, where the vertical coordinate x has its origin at the top of the filter). Assuming that the distribution of the water in the aerosol is uniform, the steady-state flow rate $G(x)$ through a cross-section of the filter at height x is proportional to the length of fiber above this point x. Thus

$$G(x) = G_F \frac{x}{L_F}, \tag{1}$$

where G_F is the mass of water droplets per unit volume of the carrier gas in unit time, and L_F is the length of the fiber. This assumes a complete removal of water from the gas by the filter, an assumption which is supported by the high efficiencies of the device.

Laminar flow in thin films was extensively studied by Levich (1962), and his approach to the slow-state motion of a film may be applied here. Using y as a radial coordinate about the center of the fiber, but with its origin on the fiber surface, the vertical velocity profile w within the film can be shown to be of the form (Agranovski, 1995)

$$w = gy\left(\delta - \frac{y}{2}\right)\Big/\nu \tag{2}$$

where $\delta = \delta(x)$ is the thickness of the film at distance x down the fiber, g is the gravitational acceleration, and ν is the kinematic viscosity of water. This is the familiar parabolic profile found in steady viscous flow, and called Poiseville flow (Levich, 1962). Such a velocity profile satisfies a no-slip condition on the surface of the fiber. Then the average velocity over a cross-section of the film at height x is

$$\bar{w} = \frac{1}{\delta}\int_0^{\delta} w\,dy = \frac{g\delta^2}{3\nu} \tag{3}$$

and the volumetric flow through the cross-section is

$$V = 2\pi r \delta \bar{w}, \tag{4}$$

where r is the radius of the fiber. Equating the flow rates in Eqs. 1 and 4 leads to

$$\delta(x) = \left(3G(x)\nu/\left(\rho_L^2 g\right)\right)^{1/3}, \tag{5}$$

where ρ_L is the density of the liquid.

To calculate the pressure drop ΔP across the filter, Kuwabara (1959) obtained an equation for the pressure drop across a filter, which becomes for $Kn = 0$ (where Kn is the Knudsen number)

$$\Delta P = \frac{4\mu_g cUH}{R^2\left(c - \frac{3}{4} - \frac{1}{2}\ln c - \frac{c^2}{4}\right)}, \tag{6}$$

where H is the thickness of the filter, μ_g is the dynamic viscosity of the gas, U is the face velocity of the aerosol, R is the effective radius of the fiber, and c is the packing density.

In practical filtration, the variable thickness of the liquid film on the fibers leads to the values of $R = R(x)$ and $c = c(x)$ which are different in the various sections of the filter. These variations affect the flow field of the gas and lead to variation in the face velocity $U = U(x)$ of the gas from section to section in the vertical direction. Note that Eq. 6 can be rewritten in the form

$$U = \frac{\Delta P R^2\left(c - \frac{3}{4} - \frac{1}{2}\ln c - \frac{c^2}{4}\right)}{4u_g cH}. \tag{7}$$

According to the classic theory of filtration, if the total single-fiber efficiency is known, the overall efficiency of a filter can be determined (Hinds, 1982; Lee and Lui, 1982a,b). The single-fiber efficiency η is usually calculated by addition of the efficiencies of the single-fiber mechanisms, that is, interception η_R Brownian motion or diffusion η_D, inertia η_I, and settling, as well as a diffusion, interception interaction term η_{DR}.

At a practical level of accuracy, the mechanisms of inertia, diffusion and settling predominate for different conditions of particle size and face velocity. For the range of velocities from 0.7 to 1.7 m/s, the particle collection due to settling is negligibly small and was not considered. The other mechanisms

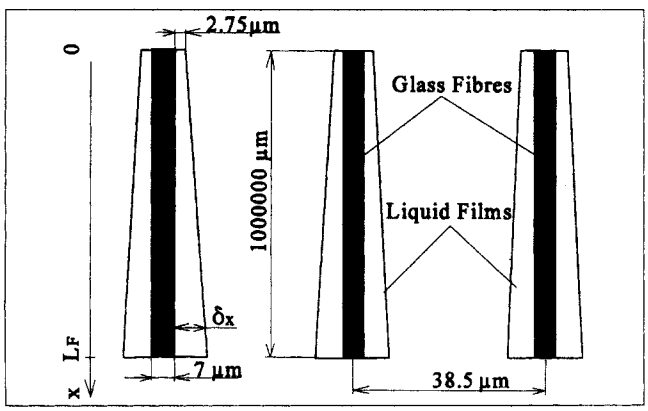

Figure 4. Conceptual fibers and liquid film.

can be considered to be mutually exclusive and they can be combined by arithmetic sum (Hinds, 1982; Kirsch and Stechkina, 1978), that is

$$\eta = \eta_I + \eta_R + \eta_D + \eta_{DR}. \tag{8}$$

In estimating the overall single-fiber collection efficiency, it is necessary to include an interaction term η_{DR} to account for enhanced collection due to interception of the diffusing particles (Hinds, 1982). Appropriate formulae are given in Hinds (1982). Once the single-fiber efficiency is known, the theoretical total filter efficiency E_T can be estimated using

$$E_T = 1 - \exp\left(-\frac{2\eta c H}{\pi r}\right), \tag{9}$$

where c is the packing density, H is the thickness of the filter, and r is the radius of the fiber (Hinds, 1982).

Experimental Studies

An experimental program was carried out to investigate the properties of the thin films on the fibers, and to assess the films' effects on the efficiency of the filtration.

Average thickness of the residual film

Two experimental techniques were employed to measure the average thickness of the residual film. In the first technique, a filter was inserted in the filter box with the fibers oriented vertically, and the plant was run until the equilibrium film had been established, that is, to the end of stage 4 as described above. Plant settings were a velocity of 1 m/s, humidity of 85%, temperature of 20°C, and with a water aerosol concentration of 3 g/m^3. The plant was then turned off and the filter allowed to drain for about 2 h until the residual film had developed. This was done in a 100% humid atmosphere to prevent evaporation losses. Then, a single fiber was carefully removed from the filter and fixed in a holder. A single dry fiber was also placed into the holder, and in the same plane as the wet fiber. The dry fiber served as a scale factor and the location reduced any parallax errors in the observation.

At the next stage, one fiber was carefully removed from the filter and fixed in a special holder. As a scale factor, a dry fiber was then placed in contact with the wet one to prevent any parallax error from the location of the fibers in different planes. The two fibers were then photographed (Figure 5) and the thickness of the liquid film was measured. Twelve experimental runs were made to determine the diameter of the residual film (see Table 1).

A second technique was developed using the full filter to provide a check on the results. As noted earlier, the filter was weighed dry and was assumed to consist of a large number of essentially parallel cylinders in a regular array. The filter had dimensions of 1 m × 30 cm × 6 mm.

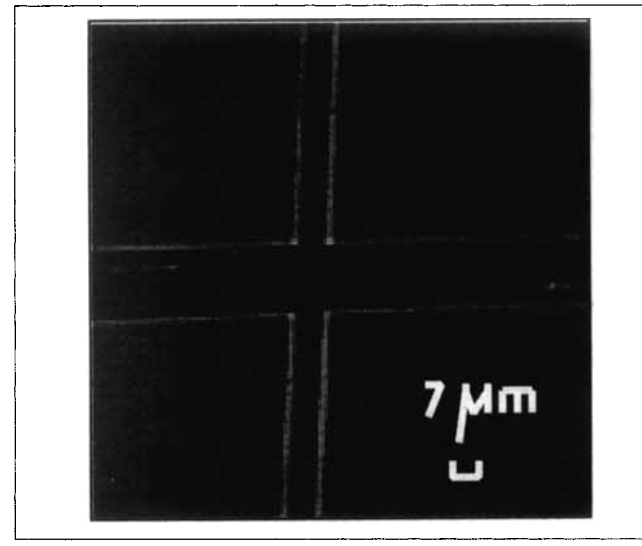

Figure 5. Image of the wet and dry fibers.

The filter was immersed in water at 20°C for 2 h to ensure it was thoroughly wet. The filter was then removed and suspended with the fibers oriented vertically in a chamber at 100% humidity and allowed to drain. This period was sufficiently long for the residual film to be fully established The wet filter was then weighed. The thickness of the residual film was determined from the difference in wet and dry weights, and the length of the fiber in the filter. This experimental procedure was repeated 12 times (see Table 1).

Effect of orientation

The theory described above relates to the case when the parallel fibers of the filter are oriented vertically. This alignment permits gravitational forces to act along each fiber and to draw water downwards through the thin film. The filters may also be mounted in the filter box with the fibers being oriented horizontally, and then the aerosol can be passed through this horizontal arrangement. In this horizontal case, gravity acts perpendicular to the fibers, and there are no preferred drainage paths for the collected liquid to follow. The horizontal arrangement will lead to drop formation and subsequent detachment.

An experiment was conducted to investigate the effect of the alignment, vertical or horizontal, on the resistance or pressure drop across the wettable fiber filter. Filters were mounted in the normal vertical alignment in the filter box, and the aerosol generator and plant were run to the end of stage 4, where the equilibrium films were fully developed.

Table 1. Film Thickness for Microscopic Analysis and for Comparison of Wet and Dry Weights

Technique	Thickness of Residual Film, μm											
Microscopic analysis	2.74	2.71	2.75	2.73	2.77	2.75	2.76	2.75	2.75	2.74	2.75	2.78
Dry vs. wet filter wts.	2.76	2.73	2.74	2.72	2.76	2.74	2.77	2.8	2.73	2.76	2.73	2.74

With the plant and aerosol still running, the pressure drop across the filter, averaged over the area of the filter, was measured. These experiments were conducted for gas velocities of 1, 2, 3 and 4 m/s, and also for aerosol concentrations of 2 g/m^3 and 4 g/m^3. Then, the filter was removed, turned through 90°, and the same experiments were repeated with the fiber alignment being horizontal. The plant and aerosol generator were run to equilibrium, where the aerosol was collecting in droplets on the filter and then detaching and falling. The average pressure drop was measured. The experiments were conducted for the same flow settings as above.

Face velocity field

The tapering of the fluid film on the vertical fiber will affect the flow field of the gas in the filter, and produce vertical differentiation of the filtration process. To quantify this effect, the test filter (mounted in the vertical orientation) was conceptually subdivided into 10 sections, each 20 cm in height and 15 cm in width, and arranged in two vertical columns of five sections in each. These sections were numbered from 1 to 10, with one column consisting of sections numbered 1, 3, 5, 7, and 9, the other column containing the even-numbered sections, and starting from the top of the filter.

The experimental plant was then run to equilibrium using an input gas velocity of 1.2 m/s, 85% humidity, 20°C, and an aerosol concentration of 3.2 g/m^3. The average pressure drop across the filter was 860 Pa. The face velocity for each of the 10 sections of the filter was measured using vane anemometers. These measurements were taken at various times: at initiation, after 1 min, 5 min, 10 min, 30 min, and 60 min of running the plant.

Efficiency

The efficiency of a filter is given by (Hinds, 1982)

$$E = 1 - \frac{\text{Final particle concentration}}{\text{Initial particle concentration}}, \qquad (10)$$

and this may be estimated by direct measurement of the initial and final particle concentrations (before and after the filter). Particle concentrations were measured using the Malvern particle-size analyzer (operating size range 0.5–650 μm) in combination with a particle counter, and the cascade impactor (operating size range 0.2–20 μm). Measured efficiencies were obtained for the size range 0.5–20 μm, which is common to both instruments.

The efficiency was measured for each of the 10 sections of the filter, as discussed above. These measurements were taken only when the equilibrium state had been reached.

Results and Discussion

The experimental results reveal some of the properties of the liquid films and their effect on the filtration efficiency.

Average thickness of the residual film

The average thickness of the residual film was measured using both a single fiber and also a complete filter. The results of 12 replicates for each technique are given in Table 1. The average film thickness is 2.75 μm.

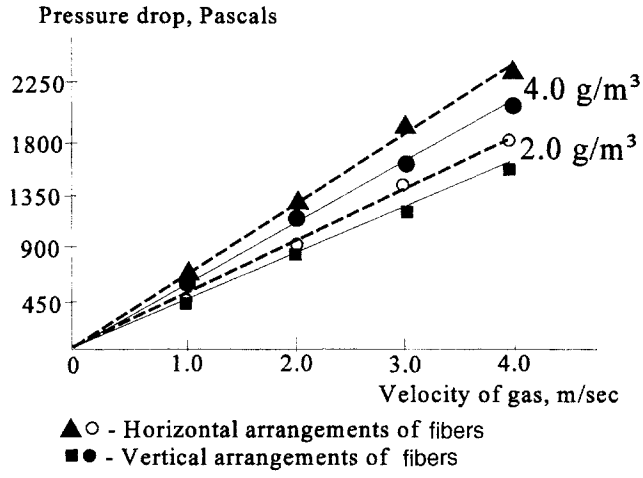

Figure 6. Pressure drops across the filter for two orientations.

Effect of orientation

The results for the experiment involving vertical and horizontal orientations of the filter are shown in Figure 6. The uninterrupted lines represent the average pressure drop across the filter in the vertical orientation, while the broken lines are the average pressure drop for the horizontal orientation. The pressure drop, or resistance, increases linearly with the velocity. The pressure drop for the horizontal orientation is larger than that for the vertical orientation for all flow velocities, and the difference also increases with flow rate. The increased pressure drop, or resistance, for the horizontal orientation is likely to be due to the less facile drainage from the horizontal fibers, the extra water on the fiber serving to block the flow of air through the filter.

Results for the face velocity field

The results for the measurement of the face velocities are shown in Figure 7, which shows the velocities in each section over time. The results in sections across the columns are consistent and show few lateral variations. The graphs show a gradation from the uniform field for the dry filter to the more structured profile when the fluid films are fully developed. There is little change to the results from 30 min to 60 min, indicating that the equilibrium film has fully developed by the 30-min mark. Taking account of the odd-even numbering of the sections, the velocity is approximately linear with height down the filter.

Efficiency

The results for the measurement of the efficiency for Sections 1–2, 5–6, and 9–10 are shown in Figure 8 and the results for some of the sections have been omitted. A cumulative size distribution of aerosol particles is shown in Figure 9. For the larger size aerosols, the measured efficiencies are

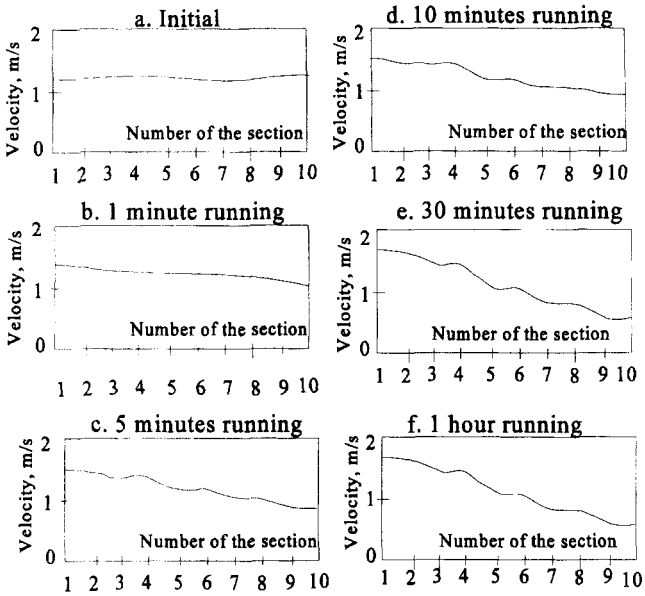

Figure 7. Face velocities of filtration in the vertical sections.

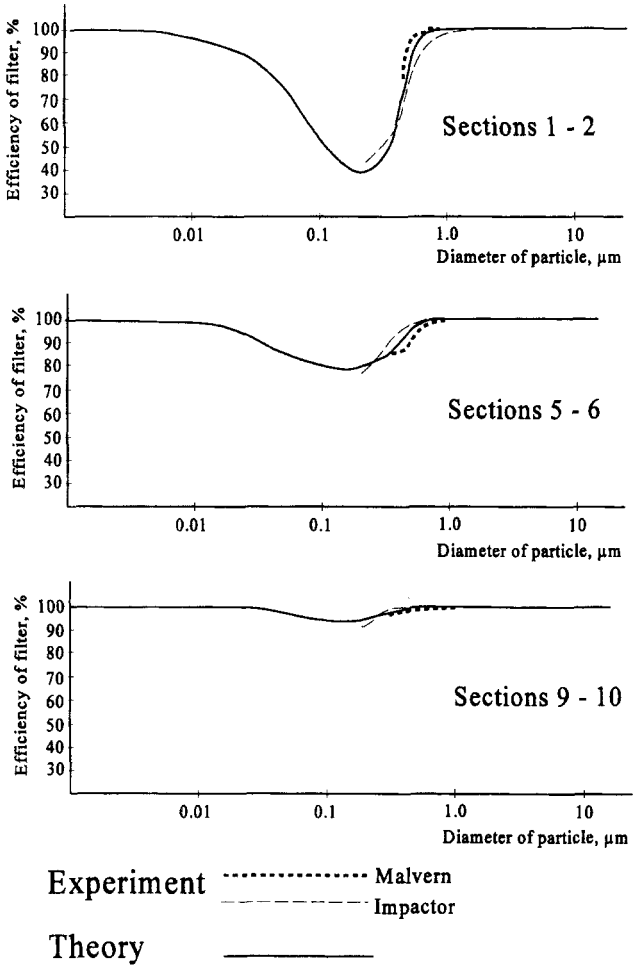

Figure 8. Overall efficiency of filtration for different sections of the filter.

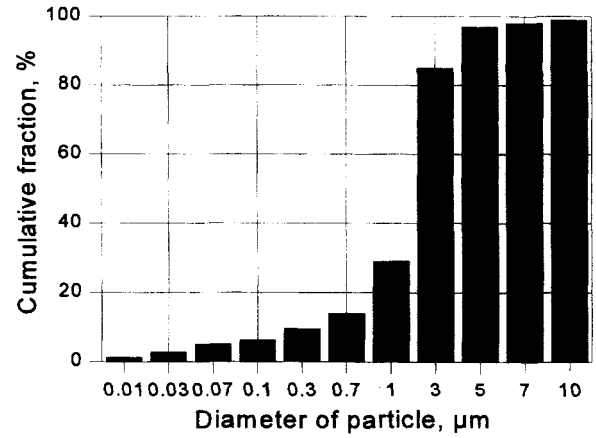

Figure 9. Cumulative size distribution of particles on filter's inlet.

nearly 100% and the results from each instrument are so close that the figure is not able to show the differentiation. There is some differentiation between the experimental results for aerosol sizes below 1 μm. The results indicate that the efficiency increases down the filter, and the effect is particularly evident for the smaller aerosol sizes.

The theoretical results in the Experimental Studies section of this article can also provide information about the filtration processes of the wet fibers. Equation 5 yields an expression for the thickness of the equilibrium film, and this is shown in Figure 10, where a logarithmic scale has been used for $G(x)$. Once wet, the film cannot be thinner than the residual thickness of 2.75 μm. Thus, there is a lower end correction factor which is shown in Figure 10, which needs to be applied to the filter, since the neighboring tapering columns (as shown in Figure 4) can merge near the bottom. For the filter used in these experiments, this limit is 15.75 μm, which corresponds to a maximum value of $G(x)$ of 79.4 g/(m·s). There is also an upper end correction factor.

Now these calculated film thicknesses can be used to estimate the local packing density of the sections of the filter. The same sections as introduced in the experimental work will be used here. The thickness of the liquid film on each fiber within a section was assumed to be equal to the calculated thickness of the film at the midpoint of that section

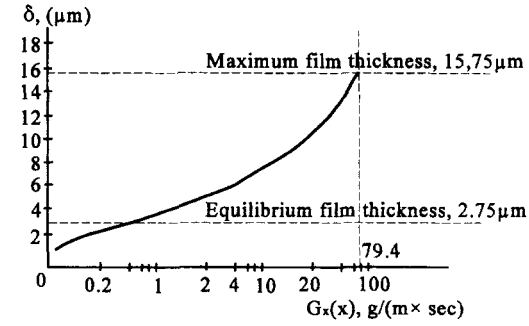

Figure 10. Thickness of the film as a function of $G(x)$.

Table 2. Calculated Packing Densities and Face Velocities

	Filter Section				
	1 and 2	3 and 4	5 and 6	7 and 8	9 and 10
Film thickness, μm	12.96	14.3	16.0	17.4	17.8
Packing density	0.103	0.125	0.157	0.185	0.193
Face velocities, m/s	1.684	1.42	1.105	0.92	0.87

using Eq. 5. The effective radius of the fiber can be used to estimate the packing density of the filter using the assumed structure shown in Figure 1.

The results are shown in Table 2, which lists the average film thickness and the average packing density by section down the filter. The packing densities vary by a factor of two from the top to the bottom of the filter. Using the average pressure drop of 860 Pa, Eq. 7 can then be used to estimate the face velocities for each sector: the results are also shown in Table 2. This shows a substantial reduction in the face velocity from the top to the bottom of the filter. Note that these calculations are based on various approximations, that is, that the sections are small enough that the film thickness varies approximately linearly across it, that the aerosol supply is uniform across the filter, and that evaporation or condensation effects are negligible.

The fully developed flow field and experimental results at 60 min (see Figure 7) can be compared with the theoretical estimates of the flow field from Table 2; these are compared in Figure 11. The variation of the collection rate due to the variation of face velocity of filtration in the vertical direction was assumed to be negligibly small. This assumption is supported by the information about size distribution of particles on the filter's inlet used in this project (Figure 9). Most particles have diameters from 0.7 to 3 μm and were removed with the efficiency higher than 98% by all sections of the filter.

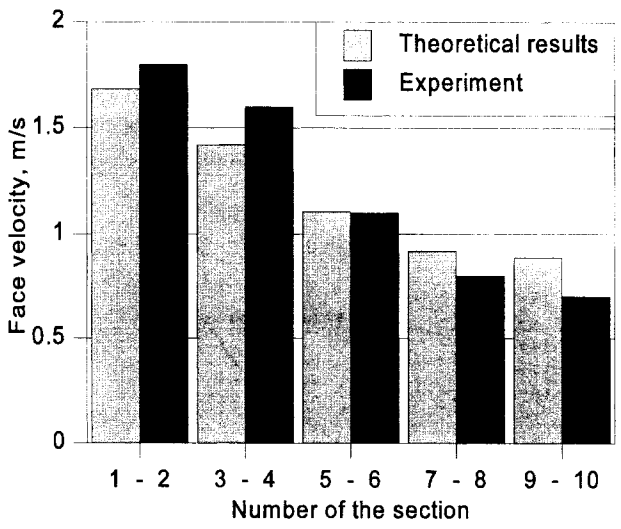

Figure 11. Face velocities of filtration, both theoretical and experimental, at the steady state (after running for 60 min).

The measured face velocities are larger than the theoretical values for the sections near the top of the filter, but the position is reversed near the bottom of the filter. This could be explained by some accumulation of water at the bottom of the filter where it attaches to the holding frame. It may also be due to some imperfections in the vertical structure of the real filter. Generally, the discrepancy between the theoretical and experimental results does not exceed 10%, and the agreement is satisfactory for most practical purposes.

Finally, the efficiency of the filter may be estimated using Eq. 9 and formulae given by Hinds (1982). The collection efficiency of the single fiber was calculated assuming that the effective diameter varied with height in the filter, that is, by using Eq. 5. The results of these calculations for Sections 1–2, 5–6, and 9–10 of the filter, for various aerosol sizes, are shown in Table 3. The single fiber efficiencies are much higher in the top sections of the filter than for the bottom sections. This arises because of the higher gas velocity through the top sections where the packing density is smaller. These theoretical results are also given in Figure 8 as the solid line. Here, the agreement between the experimental and theoretical results is excellent. The theoretical approach can also be extended to smaller aerosol particle sizes. The maximum penetration of the filter occurs for particles in the size range of 0.2–0.7 μm diameter particles. This is shown by the theoretical curve and supported by the experimental results which only partially cover the appropriate range of sizes. This maximum penetration effect arises, because the diffusional and inertial mechanisms of filtration are relatively inefficient for aerosol particles in this size range. As is evident in Figure 8, the total efficiency increases for the bottom sections of the filter.

Table 3. Single-Fiber Efficiency for Sections of Filter

Particle Size Dia., μm	η_R	η_I	η_D	η_{DR}	η
Section Nos. 1 and 2					
0.001	0.0	0.0	0.292	0.0071	0.2991
0.01	0.0019	0.0	0.034	0.002	0.0379
0.05	0.0087	0.0	0.011	0.0009	0.0206
0.1	0.017	0.000036	0.0019	0.0004	0.0193
0.5	0.092	0.026	0.0	0.0004	0.1184
1.0	0.32	0.145	0.0	0.0003	0.4653
5.0	1.24	4.41	0.0	0.0005	5.65
10.0	1.29	17.8	0.0	0.0005	19.1
Section Nos. 5 and 6					
0.001	0.0	0.0	0.385	0.008	0.393
0.01	0.0024	0.0	0.055	0.0021	0.0595
0.05	0.012	0.0	0.014	0.0009	0.0269
0.1	0.022	0.00008	0.0025	0.0005	0.0251
0.5	0.13	0.0169	0.0	0.0005	0.1474
1.0	0.41	0.082	0.0	0.0004	0.4924
5.0	1.46	3.8	0.0	0.0006	5.25
10.0	1.49	15.2	0.0	0.0006	16.69
Section Nos. 9 and 10					
0.001	0.0	0.0	0.489	0.0084	0.4974
0.01	0.0031	0.0	0.068	0.0026	0.0737
0.05	0.017	0.0	0.019	0.0013	0.0373
0.1	0.033	0.0002	0.0033	0.0006	0.0371
0.5	0.149	0.0091	0.0009	0.0006	0.1596
1.0	0.452	0.067	0.0	0.0004	0.5194
5.0	1.532	3.1	0.0	0.0006	4.632
10.0	1.547	11.3	0.0	0.0006	12.847

Conclusions

Filtration of liquid aerosols by wettable fiber filters was studied by a mixture of observation, theoretical and experimental techniques. Observations indicate that a film of liquid develops on each fiber and, after some 30 min of running, establishes a self-draining, tapered equilibrium flow down each fiber. The physical properties of these films have been established by careful observation and measurement.

Thin film theory can be used to relate the thickness of the film to the application rate of the aerosol. The results indicate the vertical height at which the films coalesce and clog the lower sections of the filter. The measured efficiencies also agree very well with the results of calculations based on the theoretical results.

The self-cleaning nature of the filter has important implications in industry. The draining liquid is readily collected, and, in the filtering of toxic materials, can be led away for further appropriate processing. The aspect ratio of such industrial filters needs to be kept small so that the clogging by the draining films is kept at a minimal level.

Literature Cited

Agranovski, I. E., "Filtration of Ultra-Small Particles on Fibrous Filters," PhD Thesis, Griffith University, Nathan, Australia (1995).

Agranovski, I. E., and R. D. Braddock, *Filtration of Mists and Fibrous Filters*, Vol. 2, World Filtration Cong., Hungary, p. 733 (1996).

Brown, R. C., *Air Filtration: An Integrated Approach to the Theory and Applications of Fibrous Filters*, Pergamon Press, Oxford (1993).

Davies, C. N., *Air Filtration*, Academic Press, London and New York (1973).

Eriksson, J., S. Ljunggren, and L. Ödberg, "Adhesive Forces Between Fibres due to Capillary Condensation of Water Vapour," *J. Coll. Int. Sci.*, **152**(2), 368 (1992).

Fairs, G., "High Efficiency Fibre Filters for the Treatment of Fine Mists," *Trans. Inst. Chem. Engrs.*, **36**, 476 (1958).

Hinds, W. C., *Aerosol Technology*, Wiley, New York (1982).

Kirsch, A., "Increase of Pressure Drop in a Model Filter During Mist Filtration," *J. Coll. Int. Sci.*, **64**(1), 120 (1978).

Kirsch, A., and I. Stechkina, "The Theory of Aerosol Filtration with Fibrous Fibers," *Fundamentals of Aerosol Science*, D. T. Shaw, ed., Wiley, New York (1978).

Kuwabara, S., "The Forces Experienced by Randomly Distributed Parallel Circular Cylinders or Spheres in Viscous Flow at Small Reynolds Numbers," *J. Phys. Soc. Japan*, **14**, 527 (1959).

Lee, K. W., and B. Y. H. Liu, "Experimental Study of Aerosol Filtration in Fibrous Filters," *Aerosol Sci. Technol.*, **1**, 35 (1982a).

Lee, K. W., and B. Y. H. Liu, "Theoretical Study of Aerosol Filtration in Fibrous Filters," *Aerosol Sci. Technol.*, **1**, 147 (1982b).

Levich, V. G., *Physico-Chemical Hydrodynamics*, Prentice-Hall, Englewood Cliffs, NJ (1962).

Mohrmann, H., "Loading of Fibre Filters with Aerosols Consisting of Liquid Particles," *Staub-Reinhalt. Luft.*, **30**, 1 (1970).

Payet, S., P. Bouland, G. Madeleine, and A. Renoux, "Dynamic Filtration of Liquid Aerosols," *Proc. of World Filtration Cong.*, 617 (1990).

Manuscript received Mar. 30, 1998, and revision received Sept. 8, 1998.